International Journal of Mechanical and Production Engineering Research and Development (IJMPERD)
ISSN(P): 2249–6890; ISSN(E): 2249–8001
Vol. 10, Issue 1, Feb 2020, 589–602

Original Article

MATHEMATICAL AND EXPERIMENTAL STUDY OF DEFORMATIONS OF STEEL ROLL ROADROLLER WITH VARIABLE GEOMETRY OF CONTACT SURFACE

MIKHAIL DOUDKIN[1], MURAT SAKIMOV[2], ALINA KIM[3], MAREK MLYNCZAK[4] & YELENA DOUDKINA[5]

[1]*Professor, School of Engineering, East Kazakhstan State Technical University, Ust-Kamenogorsk, Kazakhstan*

[2]*Senior Lecturer, School of Engineering, East Kazakhstan State Technical University, Ust-Kamenogorsk, Kazakhstan*

[3]*Associate Professor, School of Engineering, East Kazakhstan State Technical University, Ust-Kamenogorsk, Kazakhstan*

[4]*Professor, Faculty of Mechanical Engineering, Wroclaw university of Science and technology, Wroclaw, Poland*

[5]*Researcher School of Engineering, East Kazakhstan State Technical University, Ust-Kamenogorsk, Kazakhstan*

ABSTRACT

The article presents an analysis of the deformable shell behavior of a road roller, the compacted material under the compacting roller of the road roller, in which the rigid circular shell of the roller is replaced by a forcefully deformable elliptical shape, which, unlike the circular design, allows variation, adjust and optimize the impact of the road roller on the material to be compacted. It is necessary to clarify the general conceptual approach adopted in the first part of this article by a nonlinear mechanical-mathematical model of elastic gently sloping arched system under the conditions of its cylindrical bend using the curvilinear coordinate x_1 ***with a confirmed simplification about the constancy of the curvature of the curve.***

KEYWORDS: Shell, Road Roller, Drum, Steel & Stress

Received: Nov 14, 2019; **Accepted:** Dec 04, 2019; **Published:** Feb 01, 2020; **Paper Id.:** IJMPERDFEB202048

1. INTRODUCTION

The mathematical interpretation of the stress-strain state of a cylindrical shell element using differential equations, considered in previous studies [1-4, 21], is an approximate one, since it is based on a flat-plate model having an initial death [4]. This simplifying assumption did not allow, with sufficient objectivity and reliability, to quantify the possible stability loss of the shell in the local area of its contact with the road surface material to be compacted. This assertion-assumption is legitimate from the point of view of the almost complete analogy of the deformation shell of a double-hinged arch under the action of a uniformly distributed load $q = const$, where, even in the linear formulation of the problem, the upper level of the critical pressure q_{kv} is determined [4, 21].

Therefore, it is necessary to clarify the general conceptual approach adopted in the first part of this article by a nonlinear mechanical-mathematical model of an elastic gently sloping arched system under the conditions of its cylindrical bend using the curvilinear coordinate x_1 with a confirmed simplification about the constancy of the curvature of the curve, and also provided that the external loads $q_p = q_p(x_1)$ and deflection $\omega = \omega(x_1)$, there are directed along the normal to the initial surface $y_1(x_1)$ [4, 21] (Figure 1).

2. MATHEMATICAL MODEL

Considering the nature of the pressure function $q_p(x_1)$ and the fixing scheme of the element shown in Figure 1 should be considered that the subcritical compressive stress σ_{ox} corresponds to the main moment state of the shell (Figure 2), in which it is necessary to take into account the bending forces [4]. For this purpose, we introduce, as in the linear theory instead of the force parameter q_p, a fictitious transverse radial load [4, 21].

$$q_p = q_p(x_1) = -\delta \cdot \sigma_{ox} \cdot \frac{d^2\omega}{dx_1^2}, \tag{1}$$

equivalent to the action of stress σ_{ox} and equal to the projection of the distributed force σ_{ox} to the direction of the normal to the curved surface (Figure 1). From equilibrium condition [5-9, 21]

$$\sigma_{ox} = \sigma_{ox}(x_1) = \left[\frac{q_p}{\delta} - \frac{E\cdot\delta^2}{12(1-\mu^2)} \cdot \frac{d^4\omega}{dx_1^4}\right] \cdot \frac{a^2}{b} == \left[\frac{q}{l_p\cdot\delta}\sqrt{l_p^2 - x_1^2} - \frac{E\cdot\delta^2}{12(1-\mu^2)} \cdot \frac{d^4\omega}{dx_1^4}\right] \cdot \frac{\pi R_c}{2\cdot E(\xi)\sqrt{1-\xi^2}}. \tag{2}$$

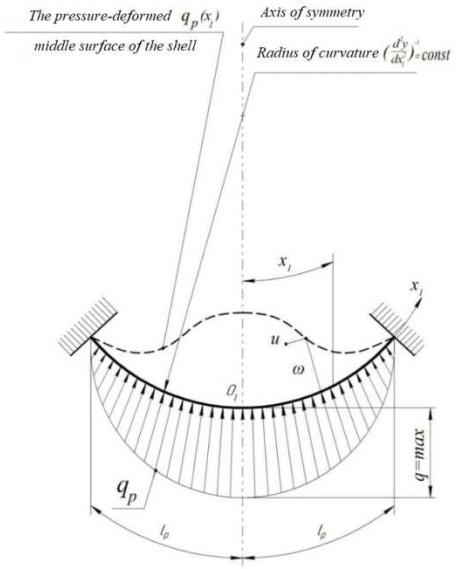

Figure 1: Refined Theoretical Design Model of the Shell Element in the Form of a Flat Cylindrical Shell-Arch [4] to Assess its Local Stability.

Replacing $q_p = \frac{q}{l_p}\sqrt{l_p^2 - x_1^2} = q\sqrt{1 - \frac{x_1^2}{l_p^2}}$ according to (1), (2), we obtain a refined-transformed nonlinear differential equation

$$\frac{E\cdot\delta^2}{12(1-\mu^2)} \cdot \frac{d^4\omega}{dx_1^4} - A\left(\frac{d^2\omega}{dx_1^2} + \frac{2\cdot E(\xi)\sqrt{1-\xi^2}}{\pi R_c}\right) + + \frac{q}{\delta}\sqrt{1 - \frac{x_1^2}{l_p^2}} \cdot \frac{\pi R_c}{2\cdot E(\xi)\sqrt{1-\xi^2}} \cdot \frac{d^2\omega}{dx_1^2} - - \frac{E\cdot\delta^2}{12(1-\mu^2)} \cdot \frac{d^4\omega}{dx_1^4} \cdot \frac{d^2\omega}{dx_1^2} \cdot \frac{\pi R_c}{2\cdot E(\xi)\sqrt{1-\xi^2}} = 0, \tag{3}$$

where the constant A is found using the same method, but using the relative deformation formula $\varepsilon_{x_1} = \varepsilon_{x_1}(x_1)$ with curvilinear coordinate x_1 [4, 21] when counting the movement $u(x_1)$ parallel to the arc l_p (Figure 1), that is

$$\varepsilon_{x_1} = \frac{du}{dx_1} - \frac{d^2y_1}{dx_1^2}\omega + \frac{1}{2}\left(\frac{d\omega}{dx_1}\right)^2 == \frac{du}{dx_1} - \frac{2\cdot E(\xi)\sqrt{1-\xi^2}}{\pi R_c}\omega + \frac{1}{2}\left(\frac{d\omega}{dx_1}\right)^2 = \frac{A}{E}; \quad (4)$$

after substituting ω and performing the integration procedure, taking into account compliance with the kinematic boundary condition $u(\pm l_p) = 0$:

$$u = u(x_1) = \int\left[\frac{A}{E} - \frac{1}{2}\left(\frac{d\omega}{dx_1}\right)^2 - \frac{2\cdot E(\xi)\sqrt{1-\xi^2}}{\pi R_c}\omega\right]dx_1 == \frac{A}{E}x_1 - 8f^2\left(\frac{x_1^3}{3l_p^4} - 2\frac{x_1^5}{5l_p^6} + \frac{x_1^7}{5l_p^8}\right) +$$

$$+\frac{2\cdot E(\xi)\sqrt{1-\xi^2}}{\pi R_c}\cdot f\cdot\left(x_1 - \frac{2x_1^3}{3l_p^2} + \frac{x_1^5}{5l_p^4}\right) + C. \quad (5)$$

Revealing obvious boundary equalities $u(0) = 0$ and $u(\pm l_p) = 0$, it is obtained (figure 1):

$$C = 0; A = \frac{16}{15}E\left(\frac{4}{7}\cdot\frac{f^2}{l_p^2} - \frac{2\cdot E(\xi)\sqrt{1-\xi^2}}{\pi R_c}\cdot f\right). \quad (6)$$

The equation (2) is calculated using the Bubnov-Galerkin method [4, 5, 9, 10], using the already known values (6) and tables of type integrals [10-12, 21]:

$$2\int_0^{l_p}\nabla_\omega(x_1)\cdot\left(1 - \frac{2x_1^2}{l_p^2} + \frac{x_1^4}{l_p^4}\right)dx_1 = 0, \Rightarrow \quad (7)$$

$$\frac{E\cdot\delta^2}{12(1-\mu^2)}\cdot\frac{64f}{5l_p^3} - \left(\frac{16}{15}\right)^2\cdot\left(\frac{4f^2}{7l_p^2} - \frac{E(\xi)\sqrt{1-\xi^2}}{\pi R_c}f\right)\times\times\left(-\frac{8f}{7l_p} + \frac{l_p E(\xi)\sqrt{1-\xi^2}}{\pi R_c}\right)E - \frac{25\pi\cdot f}{64\cdot\delta\cdot l_p}\cdot\frac{\pi R_c}{2E(\xi)\sqrt{1-\xi^2}}q +$$

$$+\frac{E\cdot\delta^2}{12(1-\mu^2)}\cdot\frac{24f^2}{l_p^3}\cdot\frac{128}{105l_p}\cdot\frac{\pi R_c}{2\cdot E(\xi)\sqrt{1-\xi^2}} = 0; \quad (8)$$

where $\nabla_\omega(x_1)$ – the left side of expression (2) in the form of a differential-algebraic operator and an additional definite integral [12, 21]

$$\int_0^{l_p}\frac{d^2\omega}{dx_1^2}\sqrt{1-\frac{x_1^2}{l_p^2}}\cdot\left(1 - \frac{2x_1^2}{l_p^2} + \frac{x_1^4}{l_p^4}\right)dx_1 =$$

$$= 4f\int_0^{l_p}\left(-\frac{1}{l_p} + \frac{3x_1^2}{l_p^3}\right)\cdot\left(1 - \frac{2x_1^2}{l_p^2} + \frac{x_1^4}{l_p^4}\right)\sqrt{1-\frac{x_1^2}{l_p^2}}dx_1 = \quad (9)$$

$$= 4f\int_0^{l_p}\left(-\frac{1}{2l_p} + \frac{5}{8l_p} - \frac{7}{16l_p} + \frac{15}{4\cdot 32l_p}\right)arcsin\frac{x_1}{l_p}\Big|_0^{l_p} = -\frac{25\cdot\pi\cdot f}{64l_p}.$$

After the term-by-term division of expression (8) into f and simple transformations, we have, in a finite explicit form, the characteristic second-order functional dependence [13-14] between q and f:

$$q = q(f) = \frac{2048}{375\pi}E\frac{\delta}{R_c}\left\{\frac{E(\xi)}{\pi}\sqrt{1-\xi^2}\left[\frac{\delta^2}{l_p^2(1-\mu^2)} +\right.\right.$$

$$+\left(\frac{16}{15}\right)\cdot\left(\frac{32f^2}{49l_p^2}-\frac{12}{7}\cdot\frac{f}{R_c}\cdot\frac{E(\xi)}{\pi}\sqrt{1-\xi^2}+\left(\frac{E(\xi)}{\pi}\sqrt{1-\xi^2}\right)^2\frac{l_p^2}{R_c^2}\right)\Bigg]++\frac{24}{21(1-\mu^2)}\cdot\frac{\delta^3 f}{l_p^4}\Bigg\}. \quad (10)$$

At $f=0$ we obtain from equality (10) the general design formula for the upper critical pressure q_{kv} [4]

$$q_{kv}=\frac{2048}{375\pi}E\frac{\delta}{R_c}\times\times\left[\frac{\delta^2}{l_p^2(1-\mu^2)}+\left(\frac{16}{15}\right)\frac{l_p^2}{R_c^2}\left(\frac{E(\xi)}{\pi}\sqrt{1-\xi^2}\right)^2\right]\frac{E(\xi)}{\pi}\sqrt{1-\xi^2}, \quad (11)$$

which is for round ($\xi=0,\ E(0)=1{,}5708$ [2]) and elliptical ($\xi=\xi_p=0{,}57, E(0{,}57)=1{,}434$ [2]) shells is written as follows:

$$q_{kv}^{(K)}=\frac{1024}{375\pi}E\frac{\delta}{R_c}\left[\frac{\delta^2}{l_p^2(1-\mu^2)}+\left(\frac{4}{15}\right)\frac{l_p^2}{R_c^2}\right]. \quad (12)$$

$$q_{kv}^{(E)}=\frac{2048}{375\pi}E\frac{\delta}{R_c}\left[\frac{\delta^2}{l_p^2(1-\mu^2)}+\left(\frac{16}{15}\right)\cdot 0{,}14066\cdot\frac{l_p^2}{R_c^2}\right]\cdot 0{,}37504. \quad (13)$$

Using the derived relations (12), (13), determine $q_{kv}^{(K)}$ и $q_{kv}^{(E)}$ at $l_p=90\ mm,\ R_c=600\ mm, \delta=6{,}5\ mm,\ E=196000\ \left(\frac{N}{mm^2}\right),\ \mu=0{,}256$ [2-7], $\pi=3{,}1416$:

$$q_{kv}^{(K)}=\frac{1024\cdot 196000\cdot 6{,}5}{375\cdot 3{,}1416\cdot 600}\left\{\left(\frac{6{,}5}{90}\right)^2\cdot\frac{1}{[1-(0{,}256)^2]}+\left(\frac{4}{15}\right)\left(\frac{90}{600}\right)^2\right\}==21{,}37\ \frac{N}{mm^2}, \quad (14)$$

$$q_{kv}^{(E)}=\frac{2048\cdot 196000\cdot 6{,}5}{375\cdot 3{,}1416\cdot 600}\left\{\left(\frac{6{,}5}{90}\right)^2\cdot\frac{1}{[1-(0{,}256)^2]}++\left(\frac{16}{15}\right)\cdot 0{,}14066\cdot\left(\frac{90}{600}\right)^2\right\}\cdot 0{,}37504=12{,}4\ \frac{N}{mm^2}. \quad (15)$$

The stability condition is observed with a large margin, as in accordance with the calculated data (14), (15).

$$\left.\begin{aligned} n_y^{(K)}&=\frac{q_{kv}^{(K)}}{q_{mp}^{(K)}}=\frac{21{,}37}{3{,}694}=5{,}8\gg[n_y]=1{,}5,\\ n_y^{(E)}&=\frac{q_{kv}^{(E)}}{q_{mp}^{(E)}}=\frac{12{,}4}{4{,}727}=2{,}62\gg[n_y]=1{,}5. \end{aligned}\right\} \quad (16)$$

Equating to zero the first derivative $\frac{dq}{df}=0$ function (104), determine the maximum deflection f_n (Figure 1)

$$f_n=\left(\frac{21}{16}\right)\cdot\frac{l_p^2}{R_c}\cdot\frac{E(\xi)}{\pi}\sqrt{1-\xi^2}-\frac{105}{(1-\mu^2)\cdot 128}\cdot\frac{\delta^3}{l_p^2}\cdot\frac{\pi}{E(\xi)\sqrt{1-\xi^2}}, \quad (17)$$

adequate lower practical load q_{kn} [4], including (at $\pi=3{,}1416$):

– for shell of circular profile ($\xi=0,\ E(0)=1{,}5708$)

$$n=\left(\frac{21}{16}\right)\cdot\frac{90^2}{600}\cdot\frac{1}{2}-\frac{105}{128}\cdot\frac{(6{,}5)^3\cdot 2}{[1-(0{,}256)^2]\cdot 90^2}=8{,}8\ mm, \quad (18)$$

– for elliptical shell ($\xi=\xi_n=0{,}57, E(0{,}57)=1{,}434$ [2])

$$f_n^{(Э)} = \left(\frac{21}{16}\right)\cdot\frac{90^2\cdot1,414\cdot0,82164}{600\cdot3,1416} - \frac{105}{128}\times\frac{(6,5)^3\cdot3,1416}{[1-(0,256)^2]\cdot90^2\cdot1,414\cdot0,82164} = 6,58\ mm. \quad (19)$$

The derived formulas (9) - (12), (17) are illustrated in Figure 2 of the existing classical curves [4] (see Table 1)

Table 1: Values of the Function (20) and (21) to the Construction of the Corresponding Graphs presented in Figure 2

f, mm	0	2	4	6	8	10	12	14	16	18	20
$q^{(К)}, \frac{N}{mm^2}$	21,37	16,43	12,74	10,32	9,2	9,31	10,7	13,37	17,38	22,52	29
$q^{(Э)}, \frac{N}{mm^2}$	12,4	9,74	8,04	7,29	7,49	8,64	10,74	13,8	17,8	22,76	28,67

$$q^{(К)} = q^{(К)}(f) = 3691,186(0,000043\,f^2 - 0,0007568f + 0,00579), \quad (20)$$

$$q^{(Э)} = q^{(Э)}(f) = 3691,186(0,0000322\,f^2 - 0,0004235f + 0,003356), \quad (21)$$

by analogy with the cubic dependencies of the simplified model. The graphs of the functional relations (20), (21), vividly characterizing the equilibrium state of the refined-modified mechanical system (Figures 1,2), along with the regular values of table 1 contain special points including upper $q_{kv}^{(К)}, q_{kv}^{(Э)}$ and bottom $q_{kn}^{(К)}, q_{kn}^{(Э)}$ extreme critical pressures

$$\left.\begin{aligned} q_{kv}^{(К)} &= 21,37\ \frac{N}{mm^2}, q_{kv}^{(Э)} = 12,4\ \frac{N}{mm^2}, \\ q_{kn}^{(К)} &= 9,08\ \frac{N}{mm^2}, q_{kn}^{(Э)} = 7,22\ \frac{N}{mm^2}, \end{aligned}\right\} \quad (22)$$

as well as corresponding movements

$$\left.\begin{aligned} f_в^{(К)} &= f_в^{(Э)} = 0, \\ f_n^{(К)} &= 8,8\ мм, f_n^{(Э)} = 6,58\ mm. \end{aligned}\right\} \quad (23)$$

It is also marked by dotted thickened lines and the maximum possible operational extremes.

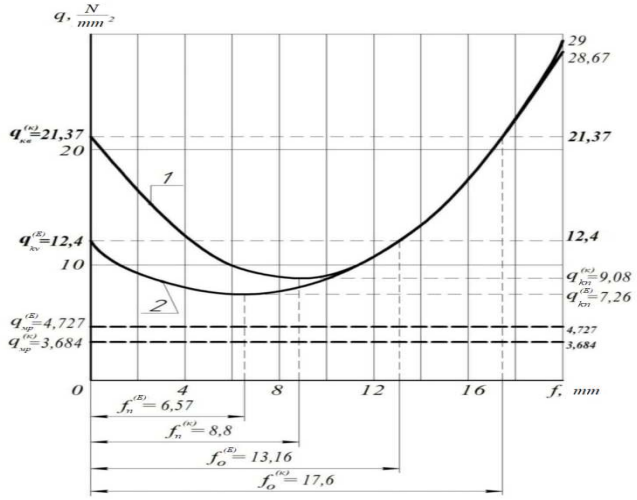

1 – Function $q^{(К)} = q^{(К)}(f)$ for round shell (20)

2 – Function $q^{(Э)} = q^{(Э)}(f)$ for elliptical shell (21)

Figure 2: Diagrams of "Load-Deflection" Corresponding to the Modified-Modified Functional Relationships (20) and (21)

$$q_{np}^{(K)} = 3,684\ \frac{N}{mm^2} = max,\ q_{np}^{(E)} = 4,727\ \frac{N}{mm^2} \tag{24}$$

To improve the accuracy of the graphic display, the deflections are also shown in Figure 7

$$f_0^{(K)} = 2f_n^{(K)} = 17,6\ mm,\ f_0^{(E)} = 2f_n^{(E)} = 13,16\ mm, \tag{25}$$

under which identities are respected

$$q^{(K)}(17,6) = q_{kv}^{(K)} = 21,37\ \frac{N}{mm^2},\ q^{(E)}(13,26) = q_{kv}^{(E)} = 12,4\ \frac{N}{mm^2}, \tag{26}$$

It is necessary to perform a condition control check [8]

$$\sigma_{0N}^{(max)} = \sigma_{0N}(0) = \frac{q_{kv}\cdot\pi\cdot R_c}{\delta\cdot 2\cdot E(\xi)\cdot\sqrt{1-\xi^2}} < \sigma_T \tag{27}$$

using formula with $x_1 = 0, f = 0,\ q = q_{kv}$confirming the physical and mathematical correctness of the refined theoretical and theoretical scheme of the cylindrical shell (Figure 1), that is, its guaranteed subcritical elasticity (without plastic deformations) during the operation of the road roller:

– in case of$\xi = 0,\ E(0) = 1,5708$(round shell shape)

$$\sigma_{0N}^{(K)}(0) = \frac{q_{kv}^{(K)}\cdot R_c}{\delta} = \frac{21,37\cdot 600}{6,5} = 1972,6\ \frac{N}{mm^2} < \sigma_T = 2270\ \frac{N}{mm^2}; \tag{28}$$

– when$\xi = \xi_p = 0,57,$ but $E(0,57) = 1,434$(elliptical shape of the drum surface [2])

$$\sigma_{0N}^{(E)}(0) = \frac{q_{kv}^{(E)}\cdot 3,1416\cdot R_c}{\delta\cdot 2\cdot 1,434\cdot\sqrt{1-(0,57)^2}} = \frac{12,4\cdot 3,1416\cdot 600}{6,5\cdot 2\cdot 1,434\cdot 0,82164} == 1526\ \frac{N}{mm^2} < \sigma_T = 2270\ \frac{N}{mm^2}, \tag{29}$$

Whence it follows that the margin of safety of the shell for the yield strength σ_m [8] varies from 13.1% to 32.8%.

The complexity of the mechanical and mathematical study of local deformations of the steel shell of a roller of a road roller with variable geometry of the contact surface and its analytical study makes it advisable to use finite element analysis, for example, using the APM FEM software package for KOMPAS-3D V17.1 [21].

Consider the results of the static calculation in KOMPAS, as well as the analysis of the stability of the elastic cylindrical shell and the results of the calculation of the natural frequencies and the change in the natural vibration forms of the thin-walled shell as a result of the machine FEM analysis according to the given data of the shell model given in tables 2, 3 and 4

It should be noted that when modeling in APM FEM, KOMPAS-3D objects must be fixed in order to prevent the free movement of the elastic shell along any of the six degrees of freedom as an absolutely rigid body [21].

Table 2: Information on Loads, Material Parameters (Steel), and the Results of the Model Breakdown into Cells

No.	Indicator	Value	№	Indicator	Value
1	Yieldpoint [MPa]	235	10	Pressure: 1	700 N
2	Elasticmodulusnormal[MPa]	200000	11	Pressure: 2	700 N
3	Poisson'sratio	0.3	12	Pressure: 3	200 N
4	Density [kg / m3]	7800	13	Itemtype	4nodaltetrahedra
5	Temperature coefficient of linear expansion [1 / C]	0.000012	14	Maximum length of the side of the element [mm]	4
6	Thermal Conductivity [W / (m * C)]	55	15	Maximumsurfacecondensationratio	1
7	CompressiveStrength [MPa]	410	16	Dilutionratioinvolume	1,5
8	EnduranceLimit [MPa]	209	17	The number of finite elements	195019
9	Torsionendurancelimit [MPa]	139	18	Numberofnodes	64262

The boundary conditions are specified with regard to symmetry, according to which the points located in the cross section of the cylindrical shell, located at a distance of half the length of the cylinder from any of the ends, cannot move along the z axis. The points located on the end of the shell are prohibited to move in the Oxy plane. Points located on a circle lying in the plane of symmetry are not allowed to move along the z axis [21].

Further, to solve the problem, a grid with finite elements was built (Figure 4). The results are contained in tables 2 and 3, and are reflected in figures 9-16.

a **b**

Figure 3: Experimental Model of a Roller of a Road Roller with an Elastic Shell, Capable of Forcibly Changing its Shape: a) Partial Assembly without Unclamping Rollers; b) Complete Assembly.

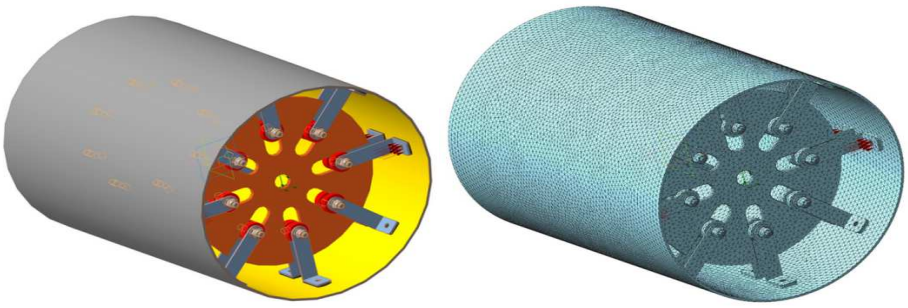

a **b**

Figure 4: Model of an Elastic, Thin-Walled Drum (a), Divided into Cells by a Finite-Element Mesh (b)

Table 3: Inertial Characteristics of the Model

No.	Indicator	Value
1	Mass of model [kg]	14.518466
2	Center of gravity of the model [m]	(-0 ; -0 ; -0.000002)
3	Moments of inertia of the model relative to the center of mass [kg * m2]	(0.566375 ; 0.392075 ; 0.392075)
4	Reactive moment relative to the center of mass [N * m]	(-0.000049 ; 0.000045 ; 0)
5	The total reaction of the supports [N]	(0 ; 0 ; -197.880822)
6	Absolutereactionvalue [H]	197.880822
7	Absolute moment value [N * m]	0.000066

Consider the results of static machine calculation in the figures.

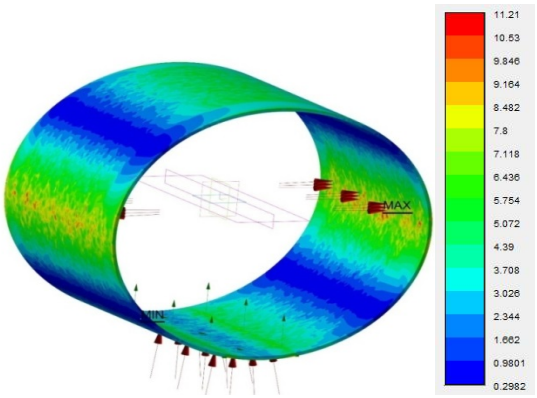

Figure 5: Distribution of von Mises Equivalent Stresses.

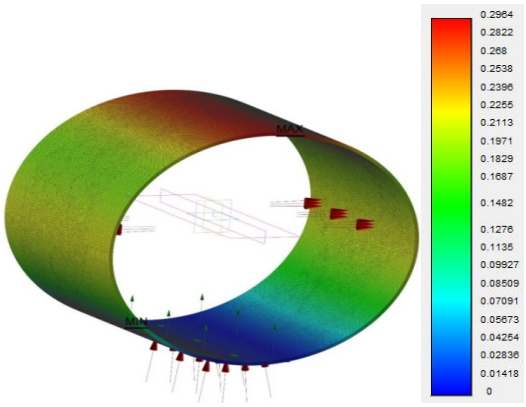

Figure 6: Total Linear Displacement.

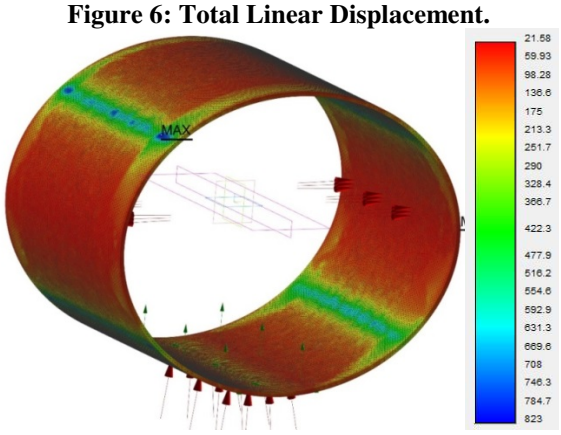

Figure 7: Action on Stress Safety Factor.

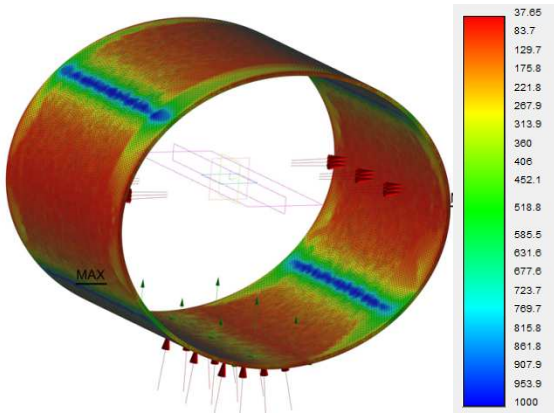

Figure 8: Distribution of Safety Factor for Strength.

In the combined figures 9-13 the possible effect on the shell of natural frequencies is consider, divided into 5 ranges (table 4).

Table 4: The Results of the Calculation of the Natural Frequencies of the Shell

No.	Frequency [rad / sec]	Frequency [Hz]
1	243.478794	38.750854
2	509.926404	81.157308
3	642.296838	102.224717
4	1432.696755	228.020771
5	1490.93104	237.289045

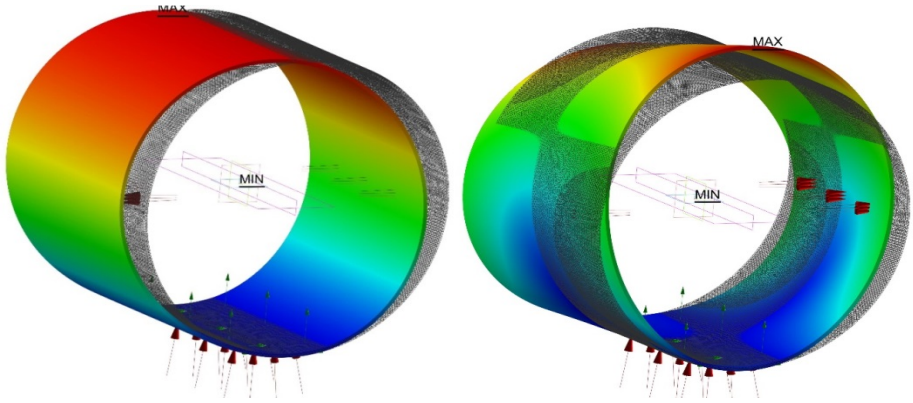

Figure 9: 1st (a) and 2nd (b) Forms of Natural Oscillations.

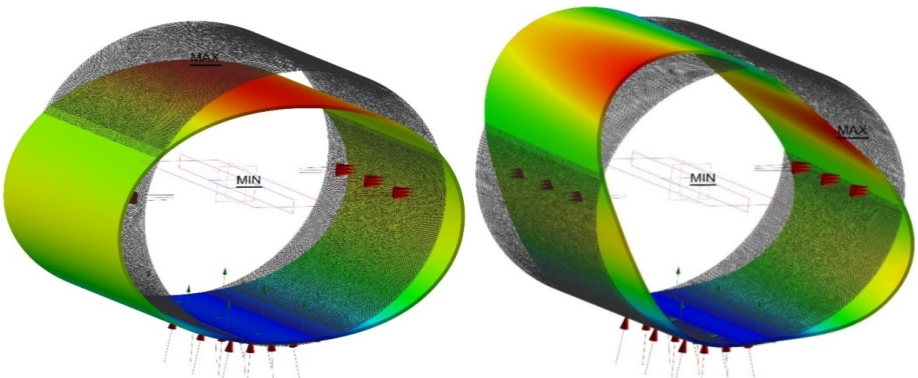

Figure 10: 3rd (a) and 4th (b) Forms of Natural Oscillations.

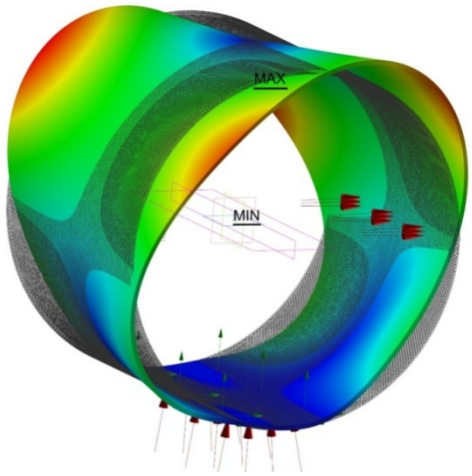

Figure 11: 5th form of Natural Oscillations of the Shell

The critical efforts obtained theoretically are several times larger than the values obtained using modeling in the APM FEM KOMPAS-3D, and therefore (as it happened) the results obtained using numerical analysis are much closer to the known experimental data than the theoretical results. This allows to conclude that a high degree of reliability of the results. This is explained by the fact that the theoretical model does not take into account, for example, the length of the elastic shell. When the grid is thickened 2 times, the critical efforts of the models obtained with the help of the APM FEM KOMPAS-3D, do not practically change. Also, the forms of buckling of a cylindrical elastic shell are almost unchanged [21].

The analysis of the tables and figures allows concluding that the solutions obtained are close to the desired exact solution, since when the grid is thickened, the values of critical forces and forms of buckling, with the exception of some curvatures, for example, in 4 and 5 forms of natural oscillations of the shell, have changed [21].

3. CONCLUSIONS

- The analysis of the research carried out allows the following conclusions to be drawn:
- the Bubnov-Galarkin variational high-precision method solved in a first approximation the original nonlinear problem of the theory of elasticity and structural mechanics of machines by definition with a margin of bearing capacity of local deformations and stability of the steel shell of a roller of a road roller with varying geometry of the contact surface compacted until the residual displacements cease [21];
- developed one-dimensional physical and mathematical models of cylindrical bending, clearly illustrated with characteristic numerical examples of a circular shell (K) and elliptical (E) outlines [2, 21] (Figures 2);
- in the process of the performed calculations, it was proved that the considered elastic element with a thickness of 6.5 mm and a radius of 600 mm was deformed within the Hooke's law at stresses of not more than 86.9% of the yield strength σ_T=2270 MPa $(\frac{N}{mm^2})$ steel grade 60C2XA [2], and theoretical safety factors $n_y^{(K)}$ =5,8 and $n_y^{(E)}$=2,62 were much higher than the minimum acceptable value $[n_y]$=1,5 [8, 21];
- it was found that to prevent the occurrence of residual deformations, local dents and clicking [4] of the shell, it is necessary to use only high-quality spring-spring steel with high $\sigma_T \geq$1800 MPa $(\frac{N}{mm^2})$ to make it, which is of great

importance in this particular case - with high requirements for fatigue strength [2, 15] and local resistance, corrosion and thermal resistance; in this regard, it is possible to recommend, for example, alloys on a cobalt-chromium-nickel base of the grades 40KXHM, 40KXHMBTU (GOST 10994-74) with $\sigma_T = 1800 \div 2500$ MPa ($\frac{N}{mm^2}$) [14-20], and also some other special structural elastically deformable steels [15] (60C2FA, 60C2XFA, 60C2XA, 65C2BA, etc.);

- the results of mathematical modeling and FEM analysis make it possible to optimize the physical and geometric characteristics of the flexible shell during its design, thereby ensuring reliable operation of the roller with an adjustable outline of the working surface of the drum, economical consumption of expensive spring-spring steel and high-quality compaction of the road surface [21].

REFERENCES

1. *Dudkin M.V., Kuznetsov P.S., Sakimov M.A., Golovin A.A., Kiyalbaev A.K. Roller of road roller. Provisional Patent RK 18131.A.S.Of the Republic of Kazakhstan No. 51084.IPC E01C 19/26, EO1C 19/23. Publ. No. 12; December 15, 2006.*
2. *Abdeev B.M., Dudkin M.V., Sakimov M.A., Eleukenov M.T. Applied theory of assessing the strength of the steel shell of the roller of a road roller with a change in the curvature of the cylindrical guide. Vestnik D. Serikbaev EKSTU. - Ust-Kamenogorsk: №4, 2011. - p. 27-36 (Part 1); №1, 2012 p. 35-45 (Part 2).*
3. *M.A. Sakimov, A.K. Ozhikenova, B.M.Abdeyev, M.V. Dudkin, A.K. Ozhiken, S. Azamatkyzy. Finding allowable deformation of the road roller shell with variable curvature. News of the national academy of sciences of the republic of Kazakhstan series of geology and technical sciences issn 2224-5278. Volume 3, Number 429 (2018), 197 – 207. http://nblib.library.kz/elib/library.kz/jurnal/Геология_03_2018/Sakimov%20(str.207)%20032018.pdf*
4. *Kolkunov N.V. Fundamentals of the calculation of elastic shells. - M .: Publishing house "High School", 1972. - 296 p.*
5. *Birger I.A., Shorr B.F., Iosilevich G.B. Calculation of the strength of machine parts: a Handbook. - M .: Mashinostroenie, 1979. - 702 p.*
6. *Ponomarev, S.D., Andreeva, L.E. The calculation of the elastic elements of machines and devices. - M .: Mashinostroenie, 1980. - 326 p.*
7. *M. Doudkin, A. Kim, V. Kim, M. Mlynczak, G. Kustarev. Computer Modeling Application for Analysis of Stress-strain State of Vibroscreen Feed Elements by Finite Elements Method. Mathematical Modeling of Technological Processes International Conference, CITech 2018, Ust-Kamenogorsk, Kazakhstan. September 25-28, 2018 Proceedings. – P. 82-96. https://doi.org/10.1007/978-3-030-12203-4_9*
8. *Mikhail Doudkin, Alina Kim, Vadim Kim. Application of FEM Method for Modeling and Strength Analysis of FEED Elements of Vibroscreen. Proceedings of the 14th International Scientific Conference on Computer Aided Engineering, June 2018. Series: Lecture Notes in Mechanical Engineering. - Wrocaw, Poland, - 2019, 892 p.*
9. *B. O. Bostanov, E. S. Temirbekov, M. V. Dudkin, A. I. Kim. Mechanics-Mathematical Model of Conjugation of a Part of a Trajectory with Conditions of Continuity, Touch and Smoothness. International Conference on Computer Aided Engineering. Computational and Information Technologies in Science, Engineering and Education, 9th International Conference, CITech 2018, Ust-Kamenogorsk, Kazakhstan. September 25-28, 2018. Proceedings. – P. 71-81.https://doi.org/10.1007/978-3-030-12203-4_8*
10. *E. S. Temirbekov, B. O. Bostanov, M. V. Dudkin, S. T. Kaimov and A. T. Kaimov. Combined Trajectory of Continuous*

Curvature. Advances in Italian Mechanism Science.Proceedings of the Second International Conference of IFToMM Italy. Mechanisms and Machine Science (MMS 68). Volume 68. IFToMM ITALY, pp. 12–19, 2019. Springer Nature Switzerland AG, 2019. ISBN 978-3-030-03319-4.https://doi.org/10.1007/978-3-030-03320-0_2

11. *M.V. Doudkin, S.Yu. Pichugin, S.N. Fadeev. Contact Force Calculation of the Machine Operational Point. Life Science Journal 2013;10(10s):246-250. (ISSN:1097-8135). Life Science Journal Editorial Office. P.O. Box 180432, Richmond Hill, New York 11418, the United States. doi:10.7537/marslsj1010s13.39. http://www.scopus.com/inward/record.url?eid=2-s2.0-84884678542&partnerID=MN8TOARS*
12. *M. V. Doudkin, S.Yu. Pichugin, S.N. Fadeev. Studying the Machines for Road Maintenance. Life Science Journal 2013;10(12s):134-138. (ISSN:1097-8135). Life Science Journal Edit. Of¬fice. P.O. Box 180432, Richmond Hill, New York 11418, the United States. doi:10.7537/marslsj1012s13.24. http://www.scopus.com/inward/record.url?eid=2-s2.0-84887523061&partnerID=MN8TOARS*
13. *Surashev, N., Dudkin, M., Yelemes, D., Kalieva, A. The planetary vibroexciter with elliptic inner race. Advanced Materials Research 694 697, 2013, pp. 229-232.*
14. *K. K. Kombayev, M. V. Doudkin, A. I. Kim, M. Mlynczak, B. K. Rakhadilov. Surface hardening of the aluminum alloys AL3 by electrolytic-plasma treatment. News of the national academy of sciences of the republic of Kazakhstan series of geology and technical sciences. Volume4, Number 436 (2019), pp. 222– 229. https://doi.org/10.32014/2019.2518-170X.117*
15. *M. Doudkin, A. Kim. G. Guryanov, M. Mlynczak, M. Eleukenov, A.Bugaev, V. Rogovsky. Process modeling and experimental verification of the conditions of ice coverage destruction of automobile roads. Journal of Mechanical Engineering Research and Developments, 42(4) 2019: 01-08 https://doi.org/10.26480/jmerd.04.2019.01.08*
16. *Andrzejczak, K., Młyńczak, M., Selech, J. Computerization of operation process in municipal transport. Advances in Intelligent Systems and Computing. 761, 2019, pp. 13-22*
17. *Giel, R., Młyńczak, M., Plewa, M. Evaluation method of the waste processing system operation. Risk, Reliability and Safety: Innovating Theory and Practice - Proceedings of the 26th European Safety and Reliability Conference, ESREL 2016. 147*
18. *Fedotov, A.I., Młyńczak, M. Analytical identification of parameters influencing measurement quality using flat brake tester. Advances in Intelligent Systems and Computing 470, 2016, pp. 147-155*
19. *Plewa, M., Giel, R., Młyńczak, M. Logistic support model for the sorting process of selectively collected municipal waste. Advances in Intelligent Systems and Computing 365, 2015, pp. 369-380*
20. *Fedotov, A.I., Młyńczak, M. Simulation and experimental analysis of quality control of vehicle brake systems using flat plate tester. Advances in Intelligent Systems and Computing 470, 2016, pp. 135-146*
21. *Mikhail Doudkin, Alina Kim, Murat Sakimov. Mechanical and mathematical research of local deformations of a steel roller shell with a variable geometry of contact surface. Production engineering archives 23 (2019) 27-35. https://doi.org/10.30657-pea.2019.25.01*
22. *Doudkin M., Apshikur B., Kim A., Ipalakov T., Asangaliyev E., Mlynczak M. Development of an installation for shear ground testing in the railway track construction. News of the National Academy of Sciences of the Republic of Kazakhstan, Series of Geology and Technical Sciences, Vol. 6, Issue 438,2019, p. 22-35. https://doi.org/10.32014/2019.2518-170X.152*
23. *Doudkin M., Apshikur B., Kim A., Ipalakov T., Asangaliyev E., Mlynczak M., Tungushbayeva Z. Development of mathematical models describing the processes occurring in the railway track construction as a whole, or in the work of its individual elements. News of the National Academy of Sciences of the Republic of Kazakhstan, Series of Geology and Technical Sciences, Vol. 5, Issue 437, 2019, p. 6-15.*

24. *Saveliev A., Zhileykin M., Mikhailovskaya V., Doudkin M., Kim A., Mlynczak M., Kustarev G., Grib V. Icreasing the reliability of the autograder metal construction by modeling and re-assembling of the working equipment. News of the National Academy of Sciences of the Republic of Kazakhstan, Series of Geology and Technical Sciences, Vol. 6, Issue 438, 2019, p. 276-286. https://doi.org/10.32014/2019.2518-170X.179*

AUTHOR'S PROFILE

Mikhail Doudkin. Doctor of Technical Sciences, Professor, School of Engineering, East Kazakhstan state technical university. He received degree of Doctor of Technical Sciences in M. Tynyshpayev Kazakh Academy of Transport and Communications, in 2010. His current research interests include road, building machines. Now he works in East Kazakhstan state technical university.

Publications 8

Murat Sakimov. Senior lecturer, School of Engineering, East Kazakhstan state technical university. His current research interests include road, building machines.

Publications 3

Alina Kim. PhD, Associate Professor, School of Engineering, East Kazakhstan state technical university. She received PhD degree in Karaganda state technical university, in 2018. Her current research interests include road, building machines.

Publications 5

Marek Mlynczak - Hab. Dr. Eng., Professor, Faculty of Engineering, Wroclaw university of Science and technology.

Publications 5

Yelena Doudkina - Researcher, School of Engineering, East Kazakhstan state technical university. Her current research interests include road, building machines.

Responsibilities:

- Management of technological processes;
- Development of technological documentation;
- Conducting research aimed at expanding the market for the sale of basic products (fibers). Certification of products;

Carrying out of experimental works on development of new technological processes, development of methods for technical control and testing of products.